DALTON
FULL PAPER

Interactions of zinc(II), magnesium(II) and calcium(II) with iminodimethylenediphosphonic acids in aqueous solutions †

Ewa Matczak-Jon,*[a] Barbara Kurzak,*[b] Anna Kamecka,[b] Wanda Sawka-Dobrowolska[c] and Paweł Kafarski[d]

[a] *Institute of Inorganic Chemistry, Wrocław University of Technology, 50-370 Wrocław, Poland. E-mail: JON@ichn.ch.pwr.wroc.pl*
[b] *Institute of Chemistry, Pedagogical University, 08-110 Siedlce, Poland. E-mail: bkurzak@wsrp.siedlce.pl*
[c] *Faculty of Chemistry, University of Wrocław, 50-383 Wrocław, Poland*
[d] *Institute of Organic Chemistry, Biochemistry and Biotechnology, Wrocław University of Technology, 50-370 Wrocław, Poland*

Received 19th May 1999, Accepted 31st August 1999

N-Substituted iminodimethylenediphosphonic acids exhibited high complexation efficiency towards zinc(II), magnesium(II) and calcium(II) ions. This results from both dinegatively charged phosphonate groups as well as the imino-nitrogen present in their structure. A significant preference for an equimolar stoichiometry and a formation of tridentate bonded species has been demonstrated in these systems. The only exception is the *N*-tetrahydrofuryl-methyliminodimethylenediphosphonic acid with a tetrahydrofuryl moiety placed in the sterically favoured position that allows its oxygen atom to be an effective metal binding site. Iminodimethylenediphosphonic and *N*-methyl-iminodimethylenediphosphonic acids behave quite differently upon zinc(II) complexation forming presumably layered two-dimensional polymeric species. These species disappear upon dilution. The crystal structure of *N*-methyl-iminodimethylenediphosphonic acid has also been determined. A unique 3-D arrangement of this compound with a tetramer as a basic building unit has been indicated.

The aminopolyphosphonic acids are multidentate complexing agents with a high specificity for various cations.[1] These compounds, synthesized for the first time in 1945 by Schwarzenbach *et al.*,[2] are now used for several purposes, mainly as scale inhibitors, in paper and textile industry, for the removal of trace amounts of metal ions from bleaching baths and in medicine as antidotes for metal overload in living organisms.[3]

The iminodimethylenediphosphonic acids, though considered as structural analogues of the popular herbicide *N*-phosphonomethylglycine (glyphosate) and of the herbicidally active derivatives of aminomethylenediphosphonic acid, show negligible herbicidal activity.[4] Since these herbicides act as inhibitors of enzymes containing metals in their active sites, the lack of herbicidal activity of iminodimethylenediphosphonic acids may originate from different complexation behaviour and co-ordination preferences compared to glyphosate or aminomethylenediphosphonic acids.

This work is aimed into aqueous solution studies of the protonation equilibria, co-ordination modes and stability of the complexes of Zn^{II}, Mg^{II} and Ca^{II} with a series of imino-dimethylenediphosphonic acids having a secondary amino moiety substituted by various functional groups. The crystal structure of *N*-methyliminodimethylenediphosphonic acid has been also determined.

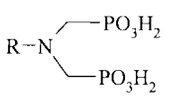

R = H	**1**
CH_3	**2**
CH_3CH_2	**3**
$(CH_3)_2CH(CH_2)_2$	**4**
(C_6H_{11})	**5**
$(C_6H_5)CH_2$	**6**
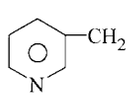	**7**
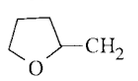	**8**

Experimental

Materials

The diphosphonic acids were obtained according to the previously described procedures.[5] Their identity was checked with the use of ES-MS spectrometry ($[M + H]^+$ for compounds **1**–**8** is at *m*/*z* 206.0, 219.8, 234.1, 276.2, 288.3, 296.2, 302.3, 290.1, respectively) and their purity was confirmed by the NMR method. The exact concentrations of the solutions of the ligands used for potentiometric studies were determined by the Gran method.[6] The concentrations of the zinc(II) and the alkaline earth metal(II) chloride stock solutions were standardised by complexometric ethylenedinitrilotetraacetate (edta) titration. Carbonate-free potassium hydroxide (the titrant) was prepared and standardised against a standard potassium hydrogenphthalate solution.

† *Supplementary data available*: rotatable 3-D crystal structure diagram in CHIME format. See http://www.rsc.org/suppdata/dt/1999/3627/

Methods

Mass spectrometry. Mass spectra were recorded in a positive-ion mode on a Finnigan Mat TSQ 700 triple quadrupole mass spectrometer operating with an ESI source. The spray voltage was 4.5 kV and the heated capillary temperature was maintained at 473 K.

Potentiometric measurements. The stability constants of the proton and metal(II) complexes were determined by pH-metric titration of 2 cm^3 samples. The ligand (L) concentration for the zinc(II) systems was 2×10^{-3} mol dm^{-3} and for the Mg^{II} or Ca^{II} 5×10^{-3} mol dm^{-3} (because of precipitation the ligand concentration for the zinc(II) systems with **6** and **7** was 1×10^{-3} mol dm^{-3}). The metal : ligand molar ratio was 1 : 1.5 and 1 : 2 and the ionic strength adjusted to 0.2 mol dm^{-3} with KCl in each case. The titrations were performed with a carbonate-free KOH solution from pH 2.5 to ≈11.5. The exception was the Zn^{II}–**1** system, where precipitation observed at pH values up to 7 prevented reliable titration curves. All titration solutions were thermostatted at 25 ± 0.1 °C using a constant-temperature water-bath.

The pH was measured with a MOLSPIN automatic titration system using a micro combination pH electrode (Mettler-Toledo, Type 2). Small amounts ($\Delta v = 0.001$ cm^3) of titrant were added (total volume = 0.1 cm^3). The electrode system was calibrated by periodic titrations of HCl solution (7.5×10^{-3} mol dm^{-3} in KCl) against standard KOH solution. The resulting titration data were used to calculate the standard electrode potentials, $E°$, and the dissociation constant for water (pK_w = 13.74). These values were then used to calculate the hydrogen ion concentration [H^+] from emf readings:[7] number of titrations, 2; total number of experimental data points used in refinement, 200; calculations were carried out using the SUPERQUAD computer program.[8] The χ^2 values never exceeded the range 5–12. The standard deviations (σ values) quoted were computed by the program and refer to random errors only. They are, however, a good indication of the importance of particular species in equilibrium.

The charges of the complexes have been omitted in the text and tables. However, for clarity, it should be mentioned that the fully deprotonated forms have negative charges L^{4-}.

NMR measurements. The NMR spectra were recorded on a Bruker DRX spectrometer operating at 300.13 MHz for ^1H, 121.50 MHz for ^{31}P and 75.46 MHz for ^{13}C, at 300 K and are given in relation to 85% H_3PO_4 (^{31}P) and $SiMe_4$, respectively. All downfield shifts are denoted as positive. The variable temperature measurements covered a temperature range of 300–350 K.

Samples for NMR studies were prepared in deuteriated water with a ligand concentration of 1×10^{-2} mol dm^{-3} and zinc(II) to ligand molar ratio of 1 : 1. Zinc nitrate hexahydrate (Aldrich) was used as a source of Zn^{II}.

The zinc(II)–L solutions were usually measured at pH above 5–6 because of precipitation. In some cases, when it was necessary to broaden the measured region of pH, we used the same concentrations of reagents as in potentiometric studies.

The complete assignments of the ^1H, ^{31}P and ^{13}C NMR spectra recorded for zinc(II) solutions with compounds **1** and **2** required shift correlated 2-D experiments. Standard programs were used to acquire [^1H, ^1H], [^{31}P, ^{31}P] as well as inverse detected [^1H, ^{13}C] and [^1H, ^{31}P] 2-D spectra. The Bruker WIN NMR DAISY software was applied to iterate ^1H NMR spectra recorded for the Zn^{II}–**1** system.

The pH of the samples was measured using a Radiometer pHM83 instrument equipped with a 2401 C combined electrode and given as meter readings without correction for pD.

Crystallography. Colourless transparent crystals (dimensions 0.2 × 0.25 × 0.3 mm) of compound **2** were grown from aqueous solution at room temperature. Their density was measured by flotation in carbon tetrachloride–ethylene bromide.

Crystal data. $C_3H_{11}NO_6P_2$, $M_r = 219.07$ g mol^{-1}, monoclinic, space group $P2_1/c$ (no. 14), $a = 7.290(2)$, $b = 8.009(3)$, $c = 14.473(2)$ Å, $\beta = 93.66(3)°$, $V = 843.3(5)$ $Å^3$ (by least squares refinement for 15 automatically centred reflections in the range of 2θ 19–25°), $Z = 4$, $D_c = 1.725$ g cm^{-3}, $T = 293$ K, $F(000) = 456$, μ(MoKα) = 0.51 mm^{-1}; 1665 independent reflections ($5 < 2\theta < 52°$) refinement on F for 1552 observed reflections ($I > 2\sigma(I)$) and 154 variable parameters. The final $R(F)$ and $wR(F^2)$ were 0.0295 and 0.0811.

The structure was solved by direct methods with SHELXS 86[9] and refined by full-matrix least-squares methods using SHELXL 93.[10]

CCDC reference number 186/1636.

See http://www.rsc.org/suppdata/dt/1999/3627/ for crystallographic files in .cif format.

Results and discussion

Potentiometric studies of proton and metal complexes

Although the fully protonated ligand forms contain five dissociable protons (H_5L^+) for **1**–**6**, **8** and six protons (H_6L^{2+}) for **7** (because of the additional proton on the pyridine nitrogen) they release only three protons in the measurable pH range ($2 < pH < 11.5$): two protons from each of the phosphonic groups (PO_3H^-) and one from the imino nitrogen, NRH^+. An additional proton from NH^+_{pyr} dissociates in **7**. The characteristic pK values for dissociation of one proton from each of the PO_3H_2 groups lie in the range 1.5–2. Thus, they do not participate in the metal co-ordination equilibria. The dissociation constants for **1** are log $\beta_1^H = 10.60(1)$, log β_2^H = 16.42(1), log $\beta_3^H = 21.28(1)$. The respective values for compounds **2**–**8** were determined previously.[11] The presence of two deprotonated phosphonic groups (PO_3H^-) in the ligand ions strongly favours formation of protonated complexes. This fact is seen in chemical models for studied systems, which contain the equimolar protonated complexes and neither 1 : 2 species (except for Zn^{II}, Mg^{II} and Ca^{II} with compound **8**) nor polynuclear species. The best fits between the measured and the calculated titrations curves have been obtained by assuming the species given in Tables 1, 2 and 3.

Zinc(II) complexes. Experimental measurements indicate that the extent of complex formation in the Zn^{II}–ligand systems is quite similar. Each sample with 1 : 1.5 metal to ligand molar ratio could be titrated without precipitation up to pH 11.5. The metal complex speciations derived from the potentiometric calculations carried out for compounds **2**–**7** do not differ considerably. Generally, the Zn^{II}–**3** system exhibits approximately the same distribution curves as those observed for ligands **2**, **4**–**7**. Therefore it can be considered as a representative for all the mentioned systems and is presented in Fig. 1(a). Obviously, the speciation of the complexes with **7** is somewhat different due to the additional proton on the pyridine nitrogen. This proton, though not participating in the co-ordination equilibria, enables formation of protonated complex. The pyridine nitrogen is unable to co-ordinate the metal ion due to steric reasons. It is interesting that the $pK_{[Zn(H_3L)]}$ value for the reaction $[Zn(H_3L)] \rightleftharpoons [Zn(H_2L)] + H^+$ is much higher (4.29) than the pK of the pyridine nitrogen of the free compound **7** (2.94). Such a significant decrease in acidity of the NH^+ of pyridine in the [$Zn(H_3L)$] complex may result from the formation of an intramolecular hydrogen bond between the pyridine nitrogen and the oxygen of the mononegatively charged PO_3H^- group. Interestingly, this effect was not observed for the system with copper(II).[11] Ligand **8** is a more effective chelating

Table 1 Zinc(II) complex formation constants (log β) of iminodimethylenediphosphonic acids at 25 ± 0.1 °C and I = 0.2 mol dm^{-3} (KCl)

	Compound						
Assignment	**2**	**3**	**4**	**5**	**6**	**7**	**8**
log β[Zn(H_3L)]	—	—	—	—	—	23.95(13)	—
log β[Zn(H_2L)]	19.58(7)	20.04(11)	20.86(7)	20.77(3)	19.80(7)	19.66(8)	20.51(2)
log β[Zn(HL)]	15.47(1)	15.78(2)	16.04(2)	16.29(1)	15.26(1)	14.92(4)	16.17(1)
log β[ZnL]	9.68(1)	9.33(3)	9.37(3)	8.67(2)	9.39(2)	9.21(4)	10.85(3)
log β[ZnLH_{-1}]	−0.25(2)	−0.22(5)	−0.20(5)	−0.54(4)	−0.20(3)	−0.47(7)	0.08(7)
log β[ZnLH_{-2}]	−11.95(5)	−11.72(9)	−11.61(9)	−9.93(6)	−11.39(5)	—	—
log β[Zn($HL)_2$]	—	—	—	—	—	—	31.10(9)
log β[Zn(HL)L]	—	—	—	—	—	—	25.34(6)
log β[ZnL_2]	—	—	—	—	—	—	15.25(5)
log β[ZnL_2H_{-1}]	—	—	—	—	—	—	3.84(6)
pK[Zn(H_3L)]	—	—	—	—	—	4.29	—
pK[Zn(H_2L)]	4.11	4.26	4.82	4.48	4.54	4.74	4.34
pK[Zn(HL)]	5.79	6.45	6.67	7.62	5.87	5.71	5.32
pK[ZnL]	9.93	9.55	9.57	9.21	9.59	9.68	10.77
pK[ZnLH_{-1}]	11.70	11.50	11.41	9.39	11.19	—	—
log β[Zn(HL)] − p$K_{(NRH^-)}$	3.72	3.58	3.74	3.79	3.94	4.52	4.71
log $K_{[ZnL]}$ − ΣpK	−12.81	−13.60	−14.01	−14.62	−12.85	−12.21	−11.53

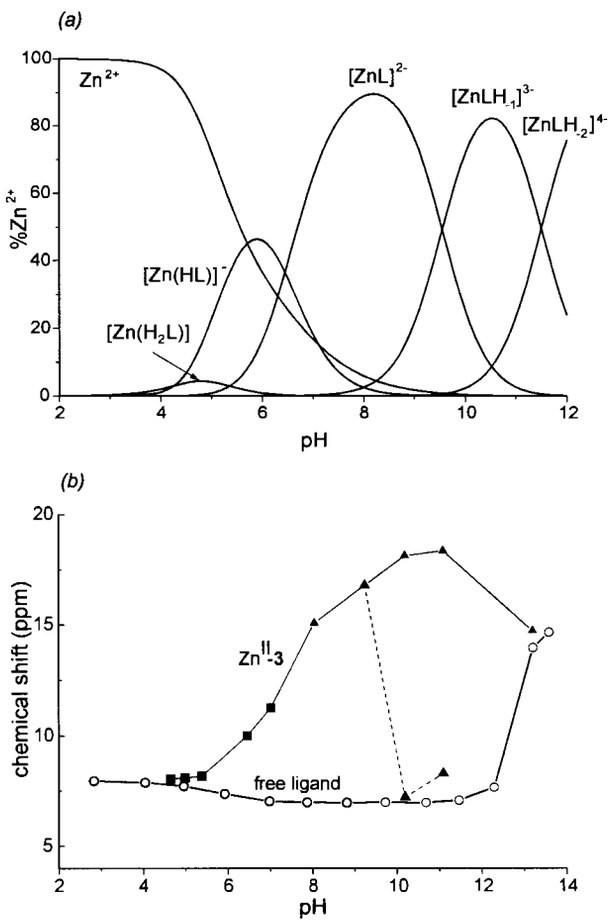

Fig. 1 *(a)* Species distribution curves for the Zn^{II}–**3** system as a function of pH simulated for conditions used in NMR studies, $c_M = c_L = 1 \times 10^{-2}$ mol dm^{-3}. *(b)* Phosphorus-31 NMR chemical shifts as a function of pH for compound **3** (○) and for Zn^{II}–**3** solutions, $c_M = c_L = 1 \times 10^{-2}$ (▲) and 1×10^{-3} mol dm^{-3} (■). Dashed line indicates upfield signals (see also Fig. 5).

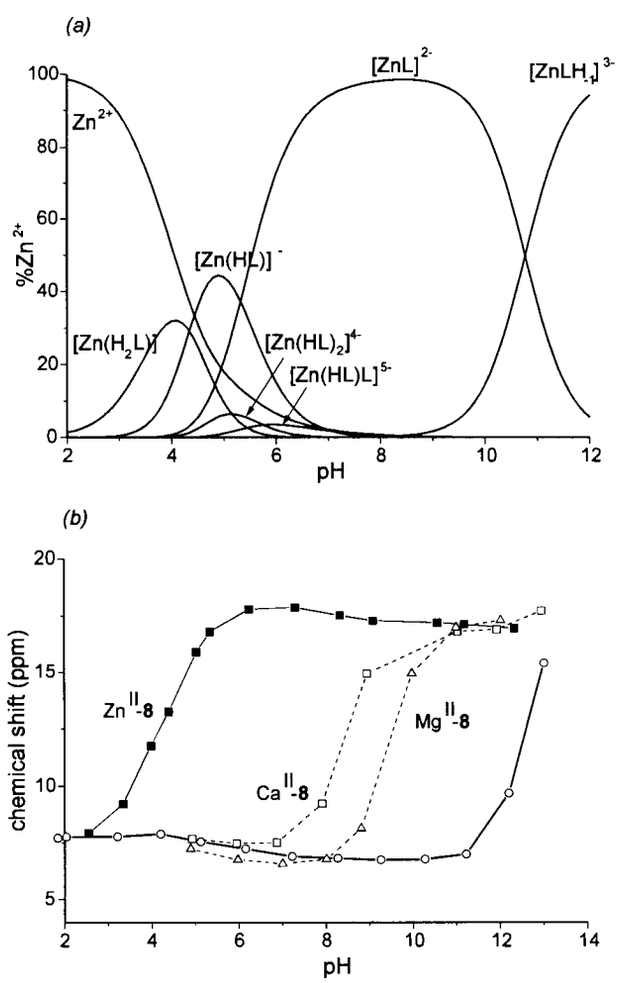

Fig. 2 *(a)* Species distribution curves for the Zn^{II}–**8** system as a function of pH simulated for conditions used in NMR studies, $c_M = c_L = 1 \times 10^{-2}$ mol dm^{-3}. *(b)* Phosphorus-31 NMR chemical shifts as a function of pH for compound **8** (○) and for Zn^{II}–**8** equimolar solution. For comparison, analogous NMR titration curves for Ca^{II}–**8** and Mg^{II}–**8** solutions, respectively.

agent than the others studied here. This is reflected in the higher basicity-adjusted stability constant, log $K_{[ZnL]}$ − ΣpK, and also in the pH value of complexation of 20% of Zn^{II}, compared to ≈5% for other ligands (see Figs. 1(a), 2(a) and Table 1).

In the presented systems only one species, [Zn(H_2L)], is formed as a minor one. The p$K_{[Zn(H_2L)]}$ values characteristic for the first deprotonation step for the [Zn(H_2L)] complexes are lower than the corresponding deprotonation constants of the "free" ligands.[11] Thus, they can be assigned to deprotonation of the phosphonic group(s) promoted by the zinc(II) binding. The

protonated ligands co-ordinate to zinc(II) by the phosphonate group(s) in a monodentate or bidentate manner. In the latter case the formation of an eight-membered chelate ring may be assumed.[12] The second deprotonation step, having $pK_{[Zn(HL)]}$ values much lower than pK_{NRH^+} of the "free" ligands, may be attributed to Zn^{II}-promoted imine nitrogen deprotonation. The first deprotonation constants of the complexes, $pK_{[Zn(H_2L)]}$, are of the same order of magnitude whereas all the second deprotonation constants of [Zn(HL)], $pK_{[Zn(HL)]}$, increase with decreasing basicity-adjusted stability constants, log $K_{[ZnL]} - \Sigma pK$, listed in the final row of Table 1.

The [ZnL] complexes are formed from [Zn(HL)] at pH *ca.* 5 and are predominant species in solution in the pH range about 7–9. The high stability constants of these species for compounds **2**–**7**, compared with those observed for simple aminophosphonates,[13] suggest tridentate co-ordination involving three donor groups. The presence of two phosphonate groups, combined with the strong metal binder, namely imino nitrogen donor, allows for a simultaneous formation of two five-membered chelate rings. It is interesting that the basicity-adjusted stability constants of the complex species with **5** and **7** behave in an opposite manner to the basicity of the "free" ligands. The probable reason for this may be that the increase of stability issuing from the ascending basicity of the co-ordinating donor groups is overcompensated by steric (R-group size) and electrostatic (polarity of the pyridine ring) effects.[14]

The chemical model for the system of ligand **8** with zinc(II) is different compared to other studied systems, due to the presence of an additional co-ordination site. A comparison of the stability constants of the complexes of compounds **6** and **8** (*i.e.* ligands of almost identical basicity) shows significant differences. The basicity-adjusted constants, log $K_{[ZnL]} - \Sigma pK$, are −12.85 and −11.53 for **6** and **8**, respectively and thus reveal a difference in stabilities of about 1.32 log units, suggesting interaction between zinc(II) and the tetrahydrofuryl oxygen atom. The sterically allowed simultaneous binding of the phosphonate O^- from the two phosphonic groups, the imino nitrogen and tetrahydrofuryl oxygen to the zinc(II) resulting in the formation of three five-membered chelate rings is reflected in the very high stability constant observed for the [ZnL] species.

For [ZnL], deprotonation processes could also be detected by potentiometry. At around pH 10.5, co-ordinated water molecules lose protons and the $[ZnLH_{-1}]$ and $[ZnLH_{-2}]$ species are formed.

It is interesting to compare the stability of the simple complex $Zn^{II} + OH^- \rightleftharpoons [Zn(OH)]$ with that of the mixed-ligand one $[ZnL] + OH^- \rightleftharpoons [ZnL(OH)]$. The equilibrium constant, $K_{[ZnL(OH)]}$, evaluated from the computed values of the related β values according to the equation log $K_{[ZnL(OH)]}$ = log $\beta_{[ZnLH_{-1}]}$ − log $\beta_{[ZnL]}$ (equilibrium 3 in Table 4 and the $[MLH_{-1}]$ species corresponds to [ML(OH)] in terms of equilibrium) shows how tightly OH^- is bound to the simple [ZnL] complex.

When we consider [ZnL(OH)] to be a mixed-ligand complex, the difference in stability, Δ log K, between the simple and mixed-ligand species is given by: Δ log K = log $K^{ML}_{[ML(OH)]}$ − log K^{M}_{MOH} = log $K^{MOH}_{[ML(OH)]}$ − log K^{M}_{ML}. The Δ log K parameter (equilibrium 5 in Table 4) expresses the effect of the bonded primary ligand (L) towards the incoming secondary ligand (OH^-). For comparison, also the log K values for the hydrolysis of both Zn^{II} and [ZnL] ions are included in Table 4. The binding strength of OH^- in mixed-ligand complexes depends on the stability of [ZnL] which, in our case, does not necessarily mean that it depends on the basicity of the ligand. In a case of bulky L bonded in the zinc(II) equimolar complex the co-ordination of OH^- is more favoured than that of the second ligand of the same kind. The formation of the higher $[ZnL(OH)_2]$ hydroxo form in solution can be explained with the high negative charge density, −4, around the metal ion forming an electrostatic cage.[15]

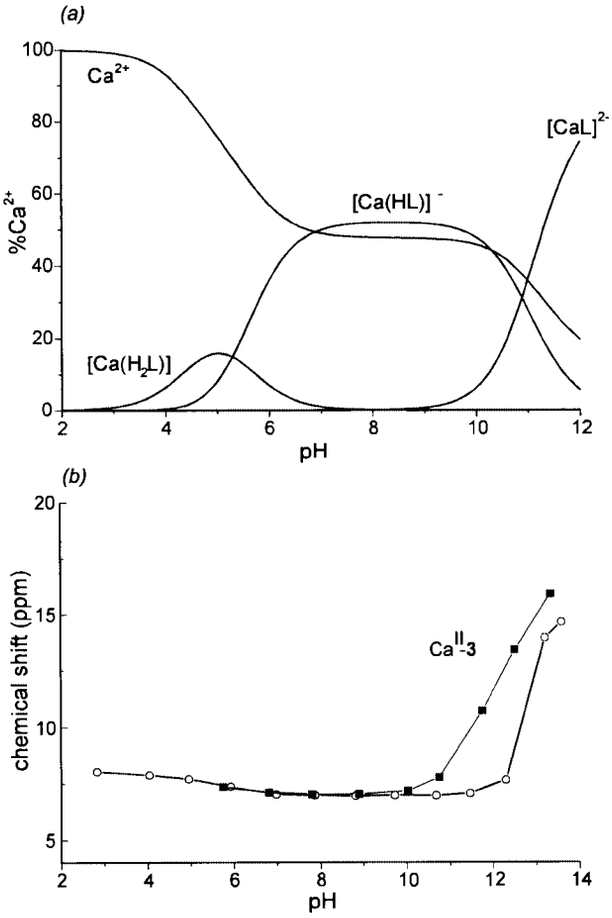

Fig. 3 *(a)* Species distribution curves for the Ca^{II}–**3** system as a function of pH simulated for conditions used in NMR studies, $c_M = c_L = 1 \times 10^{-2}$ mol dm^{-3}. *(b)* Phosphorus-31 NMR chemical shifts as a function of pH for Ca^{II}–**3** equimolar solution and **3** (○).

Magnesium(II) and calcium(II) complexes. Generally, all the distribution curves obtained for Ca^{II} and Mg^{II} with the studied ligands are approximately the same (except for those for **8**). Therefore, the Ca^{II}–**3** and Mg^{II}–**3** have been chosen as representatives for those systems and their distribution curves are presented in Figs. 3(a) and 4(a). Our experimental data for Mg^{II}– or Ca^{II}–**3** fit well with the model published by Carter *et al.*[16] The refined formation constants obtained from the best fit model data are presented in Tables 2 and 3. Calcium and Mg^{II} form [M(HL)] complexes as predominant species in the pH range 6–8.5 for **8** and 6–10 for the other ligands. This situation is quite different from that observed for the Zn^{II}–L systems in which [ZnL] is the main species in the same pH range.

The deprotonation constants, $pK_{[M(HL)]}$, of the alkaline-earth metal complexes of the studied ligands are much higher than those of the phosphonic groups and slightly lower than that of the nitrogen atom of the "free" ligands.[11] This indicates that in the [M(HL)] complexes protonation occurs on the imino nitrogen atom and the ligands co-ordinate to the magnesium(II) or calcium(II) only by the phosphonate group(s) in a monodentate or bidentate manner. The [ML] complexes start to form at pH above 10. Taking into account the difference in basicity of the co-ordinating NRH^+ group, the equilibrium constants, log $K_{[M(HL)]}$ = log $\beta_{[M(HL)]} - pK_{NRH^+}$, are approximately a 1.5 order of magnitude lower than the stability constants, log $K_{[ML]}$. This fact may indicate that in the [ML] complexes the ligands may co-ordinate by the phosphonate group(s), possibly involving also the imino nitrogen. However, the weaker tendency to metal ion promoted dissociation in the case of the calcium complexes, reflected in the slightly higher $pK_{[Ca(HL)]}$ values

Table 2 Magnesium(II) complex formation constants (log β) of iminodimethylenediphosphonic acids at 25 ± 0.1 °C and I = 0.2 mol dm^{-3} (KCl)

	Compound							
Assignment	**1**	**2**	**3**	**4**	**5**	**6**	**7**	**8**
log β[Mg(H_3L)]	—	—	—	—	—	—	23.19(3)	—
log β[Mg(H_2L)]	17.08(11)	18.72(7)	19.73(3)	20.31(2)	20.39(2)	19.03(2)	18.78(2)	19.15(4)
log β[Mg(HL)]	12.70(1)	14.16(1)	14.73(1)	15.09(1)	15.43(1)	14.13(1)	13.29(1)	14.08(1)
log β[MgL]	3.47(1)	4.74(1)	4.25(1)	4.36(1)	4.04(2)	4.34(1)	4.25(1)	5.06(2)
log β[MgLH_{-1}]	−8.29(1)	−7.42(3)	—	—	—	−7.88(2)	−7.60(3)	—
log β[Mg($HL)_2$]	—	—	—	—	—	—	—	27.16(13)
log β[Mg(HL)L]	—	—	—	—	—	—	—	18.41(14)
log β[MgL_2]	—	—	—	—	—	—	—	7.99(6)
p$K_{[Mg(H_3L)]}$	—	—	—	—	—	—	4.41	—
p$K_{[Mg(H_2L)]}$	4.38	4.56	5.00	5.22	4.96	4.90	5.49	5.07
p$K_{[Mg(HL)]}$	9.23	9.42	10.48	10.73	11.39	9.79	9.04	9.02
p$K_{[MgL]}$	11.76	12.16	—	—	—	12.22	11.85	—
p$K_{[Mg(HL)_2]}$	—	—	—	—	—	—	—	8.75
p$K_{[Mg(HL)L]}$	—	—	—	—	—	—	—	10.42
log $K_{[MgL_2]}$	—	—	—	—	—	—	—	2.93
log β[Mg(HL)] − p$K_{(NRH^+)}$	2.10	2.41	2.53	2.79	2.93	2.81	2.89	2.62

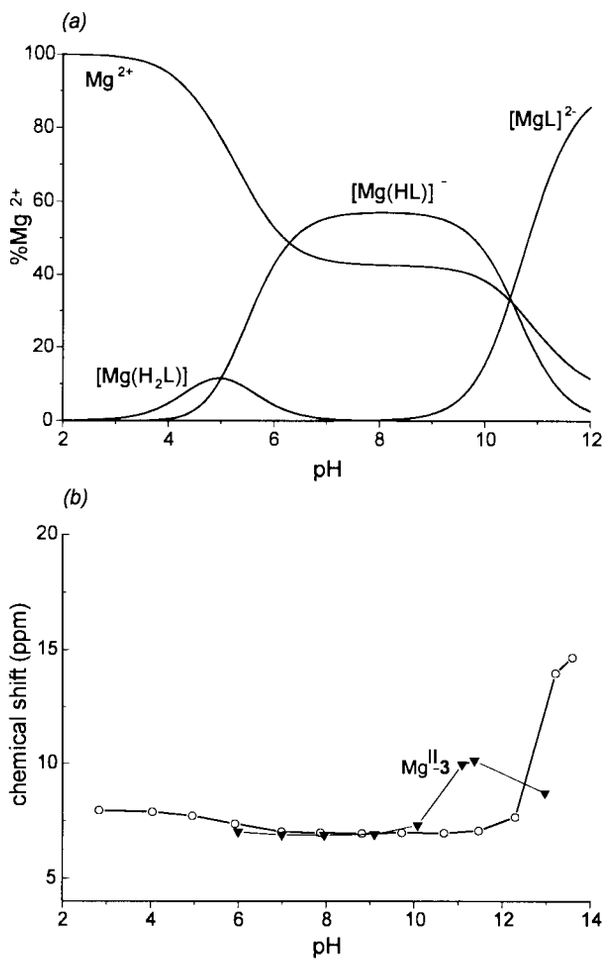

Fig. 4 *(a)* Species distribution curves for the Mg^{II}–**3** system as a function of pH simulated for conditions used in NMR studies, c_M = c_L = 1 × 10^{-2} mol dm^{-3}. *(b)* Phosphorus-31 NMR chemical shifts as a function of pH for Mg^{II}–**3** equimolar solution and **3** (○).

(compare Tables 2 and 3), suggests that nitrogen complexation in [CaL] is rather unlikely.

The complexes of Mg^{II} and Ca^{II} with compounds **6** and **8** having quite close basicity demonstrate significantly different basicity-adjusted constants, log $K_{[ML]}$ − ΣpK. Their values of −17.9 and −17.32 for Mg^{II}–**6** and Mg^{II}–**8**, and −18.36 and −16.35 for Ca^{II}–**6** and Ca^{II}–**8**, reveal a difference in stability of about 0.58 log unit for magnesium systems and 2.01 log unit for calcium systems which suggests some interactions between the metal ion and the tetrahydrofuryl oxygen, notably stronger in the case of Ca^{II}–**8**. Also crystallographic studies confirm the co-ordination ability of Mg^{II} and Ca^{II} towards the tetrahydrofuryl oxygen.[17,18]

The comparison of the pH-metric results for systems of compound **8** with Mg^{II} or Ca^{II} with those for Zn^{II}–**8** indicates that in all cases charge neutralisation favours formation of the [ML] complex with hindered co-ordination of the second ligand **8**. This tendency rises in the direction Mg^{II}, Ca^{II}, Zn^{II} which is expressed in the values of log($K_{[ML]}$/$K_{[ML_2]}$): 2.13, 3.03 and 6.45, respectively.

NMR studies

In order to obtain supporting evidence for the interpretation of the potentiometric data as well as to provide information about the metal(II) (M = Zn, Mg or Ca) binding sites we undertook NMR studies of the metal(II) solutions with compounds **1**–**8**. The ^{31}P and ^{1}H NMR spectra were measured as a function of pH for each ligand alone and in solutions containing the respective metal ion. The rates of complex formation reflected by the linewidths of the NMR signals generally followed the order Zn < Mg < Ca.

Zinc(II) complexes. The ^{31}P NMR chemical shift profiles of ligand **3** and species formed upon complexation with the zinc(II) ions are given in Fig. 1(b) together with the species distribution curves obtained from the potentiometric results. These data reveal a full consistence between the NMR and potentiometric studies and are representative for the zinc(II) systems with compounds **3**–**6**. For acidic solutions an equimolar mixture of zinc(II) with **3** exhibits δ_P values almost identical with those of the ligand. The signals are sharp indicating that exchange involving protonated forms of the ligand and the protonated complexes is fast and that only labile, short-lived in respect of the NMR timescale, zinc–oxygen bonds may be formed in the [Zn(H_2L)] and [Zn(HL)] species. Stepwise nitrogen complexation leading to the predominant, tridentate bonded [ML] followed by the [MLH$_{-1}$] species is reflected both in a gradual downfield shift of ^{31}P resonances and in a significant (about 5 log units) decrease in pK_{NRH^+}. Furthermore, the formation of two joined five-membered chelate rings involving more kinetically inert metal–nitrogen bonding results in a considerable broadening of ^{31}P signals.[19]

Table 3 Calcium(II) complex formation constants (log β) of iminodimethylenediphosphonic acids at 25 ± 0.1 °C and I = 0.2 mol dm^{-3} (KCl)

	Compound							
Assignment	**1**	**2**	**3**	**4**	**5**	**6**	**7**	**8**
log β[Ca(H_3L)]	—	—	—	—	—	—	22.83(4)	—
log β[Ca(H_2L)]	17.09(9)	19.13(4)	19.88(3)	20.36(2)	20.30(5)	19.05(4)	18.33(3)	19.00(4)
log β[Ca(HL)]	12.42(1)	14.03(2)	14.59(2)	14.89(1)	15.09(2)	13.91(1)	12.87(1)	14.01(1)
log β[CaL]	3.11(1)	4.11(1)	3.71(2)	3.77(1)	3.39(2)	3.88(1)	3.69(1)	6.03(1)
log β[CaLH_{-1}]	−8.68(1)	−8.66(10)	—	—	—	−8.68(10)	−8.49(2)	—
log β[CaL_2]	—	—	—	—	—	—	—	9.03(3)
p$K_{[Ca(H_3L)]}$	—	—	—	—	—	—	4.50	—
p$K_{[Ca(H_2L)]}$	4.67	5.10	5.29	5.47	5.21	5.14	5.46	4.99
p$K_{[Ca(HL)]}$	9.31	9.92	10.88	11.12	11.70	10.03	9.18	7.98
p$K_{[CaL]}$	11.79	12.77	—	—	—	12.56	12.18	—
log $K_{[CaL_2]}$	—	—	—	—	—	—	—	3.00
log β[Ca(HL)] − p$K_{(NRH^+)}$	1.82	2.28	2.39	2.59	2.59	2.59	2.47	2.55

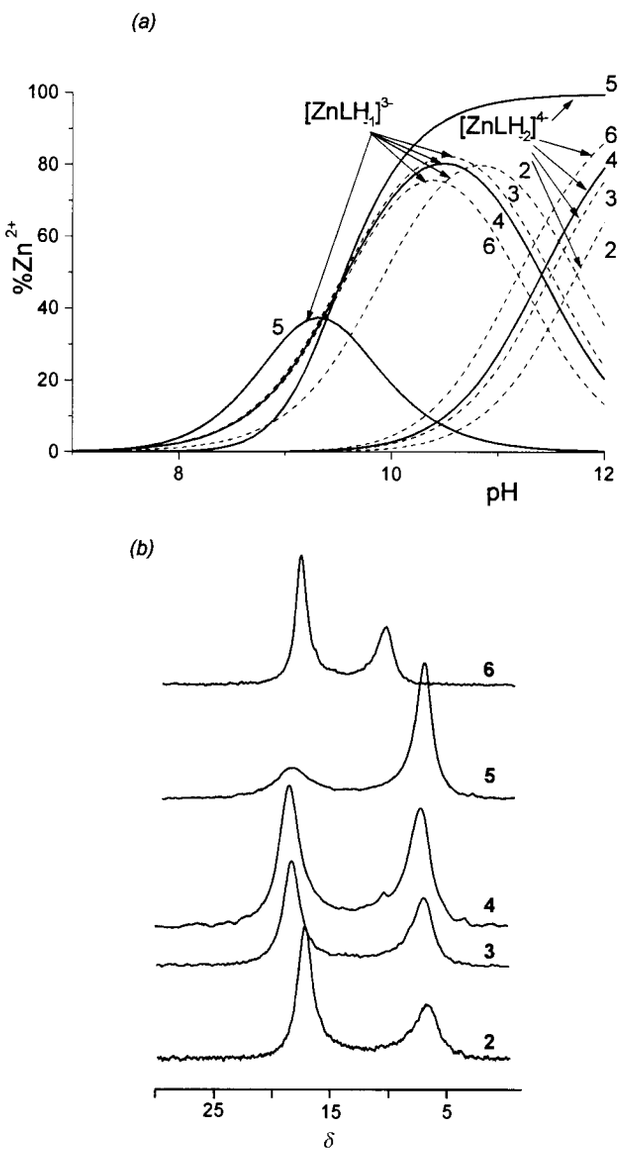

Fig. 5 Species distribution curves *(a)* and phosphorus-31 NMR spectra *(b)* for the Zn^{II}–L systems with compounds **2**–**6** revealing the formation of the [ZnLH_{-1}] and [ZnLH_{-2}] complexes (**2**, pH 11.60; **3**, pH 11.22; **4**, pH 11.76; **5**, pH 11.36; **6**, pH 12.56).

Accordingly, in the ^{1}H NMR spectra the protons of methylenephosphonate groups appearing as single doublets (J_{P-H} ≈ 11.5 Hz) are usually the most informative with respect to zinc(II) complexation. When protonated oxygen-bonded species are formed only insignificant CH_2(P) chemical shifts in the ^{1}H spectra of the ligand solutions upon addition of Zn^{II} are noted. Formation of the [ML] complex results in the appreciable upfield shifting of the CH_2(P) signal with $\Delta\delta$ corresponding to the maximum contribution of [ML] being about 0.3 ppm in respect to the HL species.

There is a narrow alkaline region (pH ≈ 11–12.5) where ^{31}P NMR spectra recorded for zinc(II) solutions with ligands **3**–**6** and **2** (see discussion below) split into two broad resonances appearing in two distinct regions of the spectra, namely at δ 17.6–19 and 6.0–11.0. The temperature dependent NMR measurements indicated their coalescence at 310–320 K followed by apparent narrowing of the resulting very broad signal. The best agreement between these spectroscopic and potentiometric data was obtained when the [MLH_{-2}] species was included in the speciation model (Fig. 5(a), 5(b)).

The most notable difference between the zinc(II) solutions of compounds **7** and **6** is the lack of corresponding, upfield ^{31}P resonances in alkaline solutions of **7** which is consistent with a speciation model assuming lack of the [MLH_{-2}] hydroxo complex. There is no spectroscopic evidence revealing involvement of pyridyl nitrogen in zinc(II) complexation.

Both the distribution diagram and the ^{31}P NMR chemical shifts depending on pH for Zn^{II}–**8** (Fig. 2) differ considerably from those for Zn^{II} with **3**–**6** (**7**) for which the Zn^{II}–**3** system was used as a representative (Fig. 1). As shown in Fig. 2(b), the pH region indicating a steep change in δ_P values moves by about 3 log units towards the acidic side compared to the respective curve obtained for Zn^{II}–**3**. This effect is considerably stronger than should be expected only from the difference in the p$K_{[Zn(HL)]}$ values of **3** and **8** which is 1.13. It may indicate that the imino nitrogen is quite tightly bonded to Zn^{II} also in [Zn(HL)] and that ligand protonation occurs on the phosphonate moiety. Hence, the complexation of Zn^{II} by the tetrahydrofuryl oxygen, resulting in a tetradentate co-ordination in both [Zn(HL)] and [ZnL], should play a significant role as a metal–nitrogen bonding stabilisation factor. This is not surprising since the co-ordination ability of the tetrahydrofuryl oxygen to Zn^{II} has been well documented.[17,20]

Quite unexpectedly, the interaction modes observed for Zn^{II} with compounds **1** and **2** appear to be significantly different from the rest. The ^{31}P NMR spectra exhibit new resonances as a pair of narrow, almost intact *versus* pH (in the range 7–10.5) doublets of similar intensity. The ^{31}P–^{31}P correlation spectra indicate that each doublet corresponds to the non-equivalent phosphonate group and both phosphorus nuclei are coupled with the J_{P-P} of 5.6 and 6.4 Hz for **1** and **2**, respectively (Fig. 6(a)). These values allow discrimination of a pyrophosphonate type bond formation since the geminal $^2J_{P-O-P}$ coupling constants lie usually in the range −10.7 to −20 Hz[21] and indicate the existence of a long-range phosphorus–phosphorus coup-

Table 4 Equilibrium formation constants of zinc(II) complexes of iminodimethylenediphosphonic acids

Equilibrium	Compound 2	3	4	5	6	7	8
1. $M + L \rightleftharpoons ML$	9.68	9.33	9.37	8.67	9.39	9.21	10.85
2. $M + H_2O \rightleftharpoons MOH + H^+$	−9.39	−9.39	−9.39	−9.39	−9.39	−9.39	−9.39
3. $ML + H_2O \rightleftharpoons ML(OH) + H^+$	−9.93	−9.55	−9.57	−9.21	−9.59	−9.68	−10.77
4. $MOH + L \rightleftharpoons ML(OH)$	9.14	9.17	9.19	8.85	9.19	8.92	9.47
5. $MOH + ML \rightleftharpoons ML(OH) + M$	−0.54	−0.16	−0.18	0.18	−0.20	−0.29	−1.38

Table 5 Spectral parameters δ and J/Hz for compounds **1** (R = H) and **2** (R = CH_3) in solutions with zinc(II) ions

R–N(CH$_2$PO$_3$H$_2$)(CH$_2$PO$_3$H$_2$)		^{31}P		^{13}C			^{1}H				
		δ_P	J_{P-P}	δ_{CH_2}	$^1J_{C-P}$	$^3J_{C-P}$	$\delta_{H(A)}$	$\delta_{H(B)}$	$J_{H(A)-H(B)}$	$J_{P-H(A)}$	$J_{P-H(B)}$
R = H	(1)	16.27	5.6	50.14	124.6	15.4	2.42	2.95	−17.5	12.5	16.4
	(2)	20.86		48.25	143.5	12.5	2.54	3.06	−17.9	13.8	16.1
R = CH_3	(1)	14.63	6.4	61.58	132.5	14.5	2.68			14.4	
	(2)	20.25		58.34	152.0	14.1	2.73			13.0	

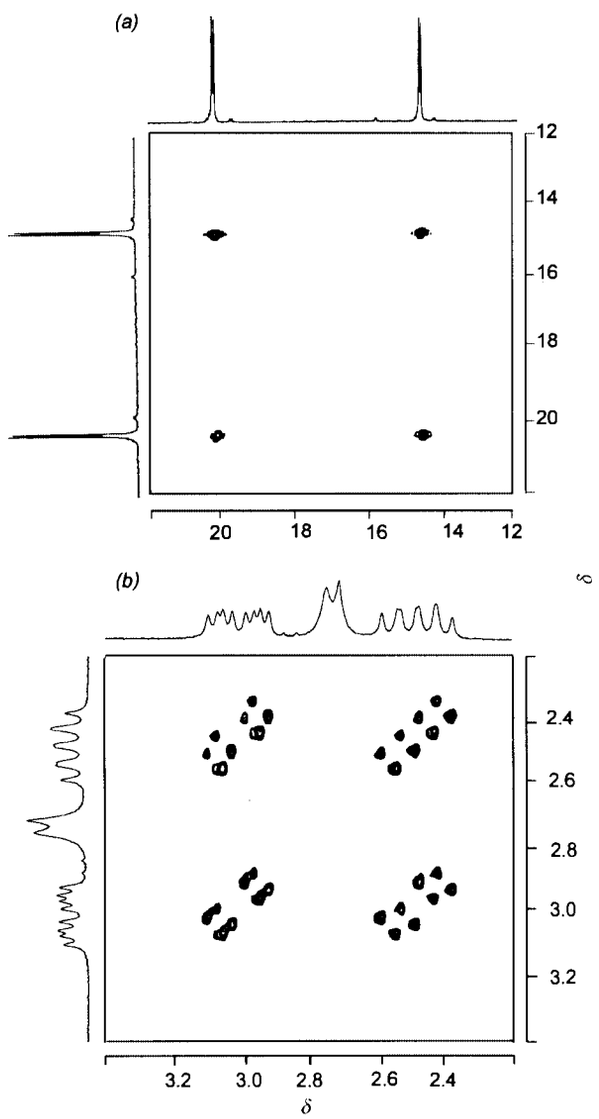

Fig. 6 The ^{31}P–^{31}P *(a)* and ^{1}H–^{1}H *(b)* correlation spectra for the Zn^{II}–**2** ($c_M = c_L = 1 \times 10^{-1}$ mol dm^{-3}, pH 9.22) and Zn^{II}–**1** ($c_M = c_L = 1 \times 10^{-1}$ mol dm^{-3}, pH 9.30) systems, respectively.

ling, most likely through four bonds. Although both the ^{31}P chemical shifts and the J_{P-P} coupling constants do not vary much from **1** to **2** there are significant differences in their ^{1}H NMR spectra. In the case of Zn^{II}–**2** the methylene CH_2(P) protons are equivalent within each non-equivalent methylenephosphonate fragment which results in separate doublets corresponding to each methylenephosphonate arm. On the contrary, the ^{1}H NMR spectrum of Zn^{II}–**1** exhibits independent ABX (X = ^{31}P) spin systems for protons of each non-equivalent methylenephosphonate group. Some amount of a [ML] complex is also indicated (Fig. 6(b)). The non-equivalence of the methylenephosphonate arms, although quite unusual, is additionally confirmed by the ^{13}C NMR spectra where each resonance of the methylene carbon atom adjacent to the phosphonate group appears as a doublet of doublets with the smaller of the two coupling constants assigned to $^3J_{P-C-N-C}$. All the signals, based on the homo- and hetero-nuclear 2-D experiments, are summarised in Table 5.

The striking feature of the described phenomenon is that the formation of the new species is strongly dependent upon the metal to ligand stoichiometry and the solution concentration. They prove to be predominant in 0.1 mol dm^{-3} solutions used in 1:1 molar ratio. The dilution of Zn^{II}–**2** leads to a stepwise disappearance of ^{31}P doublets with simultaneous appearance of a broad signal attributed previously to the [ML] complex with a tridentate ligand co-ordination. The latter signal is the only resonance in solutions where the concentration of both reagents is 1×10^{-3} mol dm^{-3} (Fig. 7). The dilution apparently leads to the [ML] species as a final complex also in the Zn^{II}–**1** system. Moreover, both the potentiometry and NMR consistently indicate formation of the [MLH_{-1}] and [MLH_{-2}] hydroxo complexes in Zn^{II}–**2** diluted solutions (Fig. 5). However, there is no spectroscopic evidence for [MLH_{-2}] formation in alkaline solutions of Zn^{II}–**1**. The variable temperature ^{31}P NMR spectra of Zn^{II}–**2** 0.01 mol dm^{-3} solutions, in which the pair of doublets as well as the signal corresponding to the [ML] complex are observed (Fig. 7(b)), indicate a difference in the temperature-dependent behaviour for both types of signals. At higher temperatures the doublet pair broadens, whereas the broad resonance apparently undergoes a significant narrowing. Furthermore, the latter signal is the only detectable resonance at 350 K.

All these observations suggest an non-typical for zinc(II) systems, slow on the NMR timescale, exchange between

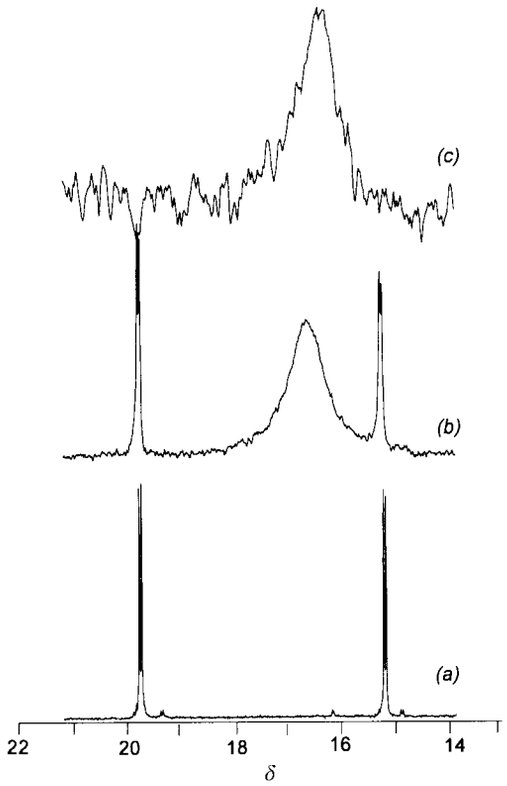

Fig. 7 The changes in the phosphorus-31 NMR spectra of the Zn^{II}–**2** system upon dilution: *(a)* $c_M = c_L = 1 \times 10^{-1}$ mol dm^{-3}; pH 8.98, *(b)* $c_M = c_L = 1 \times 10^{-2}$ mol dm^{-3}; pH 8.33; *(c)* $c_M = c_L = 1 \times 10^{-3}$ mol dm^{-3}, pH 7.24.

phosphorus nuclei being in chemically different environments. The exchange rate for this process must be significantly lower than that characterising the equilibria between [MLH_{-1}] and [MLH_{-2}] complexes (Fig. 5(b)), although the kind of spectra we obtained in the latter case is also not a common feature for zinc(II) systems. Consequently, the different ^{31}P NMR chemical shifts can be assigned to one of the phosphonate arms involved in (N, O) chelation of Zn^{II} (downfield signal) and to the second arm which co-ordinates Zn^{II} in an O-monodentate manner (upfield signal).

Magnesium(II) and calcium(II) complexes. The ^{31}P chemical shift profiles and the species distribution diagrams for systems Ca^{II}–**3** (Fig. 3(b)) and Mg^{II}–**3** (Fig. 4(b)) are generally representative for all the systems studied with the exception of that found for compound **8**. The differences in ^{31}P chemical shifts of the ligand upon complexation are relatively small in the spectra of the Ca^{II}–**3** system and larger for the alkaline region of the Mg^{II}–**3** system. The NMR data reveal protonation on nitrogen in the [M(HL)] complexes which is in a good agreement with the potentiometric results.

Sawada *et al.*[12] has suggested that both Ca^{II} and Mg^{II} form rather weak ionic M–N bonds in the complexes with the unprotonated aminophosphonates (including ligand **2**). However, our spectroscopic results seem to indicate that Ca^{II} is not complexed through the imino nitrogen in [CaL], except for the case of **8**, where the tetrahydrofuryl oxygen co-ordination additionally stabilises the complex. This is evidenced in the significant decrease of the pK_{NRH^+} when Ca^{II} is added to the ligand solution (Fig. 2). A smaller decrease of the pK_{NRH^+} of **8** is observed upon complexation with Mg^{II} (Fig. 2). This indicates that, although the ligand co-ordination in the Ca–**8** and Mg–**8** complexes is probably the same, the metal–ligand interaction is much stronger for the former. The Mg–N bonding in the [MgL] complexes with ligands **1**–**7** appears to be weaker than that with **8** and easily ruptured upon a pH increase.

Table 6 Bond lengths [Å], angles [°] and torsion angles [°] for compound **2**

P(1)–O(1)	1.5531(13)	P(1)–C(1)	1.825(2)
P(1)–O(2)	1.5122(13)	P(2)–C(2)	1.833(2)
P(1)–O(3)	1.5092(13)	N(1)–C(2)	1.503(2)
P(2)–O(4)	1.4878(13)	N(1)–C(1)	1.503(2)
P(2)–O(5)	1.5190(15)	N(1)–C(3)	1.503(2)
P(2)–O(6)	1.5642(16)		
O(3)–P(1)–O(2)	116.47(8)	O(4)–P(2)–C(2)	110.00(7)
O(3)–P(1)–O(1)	107.77(8)	O(5)–P(2)–C(2)	102.04(8)
O(2)–P(1)–O(1)	112.40(8)	O(6)–P(2)–C(2)	106.82(7)
O(3)–P(1)–C(1)	107.42(7)	C(2)–N(1)–C(1)	115.64(13)
O(2)–P(1)–C(1)	105.35(8)	C(2)–N(1)–C(3)	112.14(13)
O(1)–P(1)–C(1)	106.90(8)	C(1)–N(1)–C(3)	111.03(13)
O(4)–P(2)–O(5)	118.05(8)	N(1)–C(1)–P(1)	113.41(11)
O(4)–P(2)–O(6)	108.76(8)	N(1)–C(2)–P(2)	116.12(11)
O(5)–P(2)–O(6)	110.51(9)		
C(2)–N(1)–C(1)–P(1)	−57.0(2)		
C(1)–N(1)–C(2)–P(2)	−69.1(2)		
C(3)–N(1)–C(1)–P(1)	173.8(1)		
C(3)–N(1)–C(2)–P(2)	59.6(2)		
O(1)–P(1)–C(1)–N(1)	83.0(1)		
O(2)–P(1)–C(1)–N(1)	−157.3(1)		
O(3)–P(1)–C(1)–N(1)	−32.5(1)		
O(4)–P(2)–C(2)–N(1)	22.7(1)		
O(5)–P(2)–C(2)–N(1)	148.8(1)		
O(6)–P(2)–C(2)–N(1)	−95.2(1)		

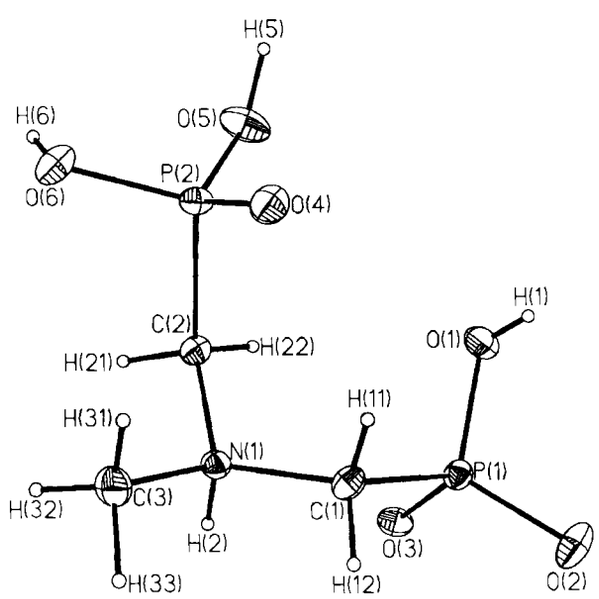

Fig. 8 The molecular structure and the numbering scheme of ligand **2**. Displacement elipsoids are shown at the 30% probability level (ORTEP II[22]).

It is also worth mentioning that the NMR titration data obtained for compounds **1** and **2** in the presence of Ca^{II} and Mg^{II} do not differ markedly from those presented in Figs. 3 and 4. These results support our earlier observation that Zn–N bond formation is an important factor responsible for the appearance of the species characterised in Table 5.

Crystal structure of compound 2

The molecular structure and atom numbering of compound **2** is given in Fig. 8. Table 6 summarises selected bond distances and angles. Similarly, as with other iminodimethylenediphosphonates described previously (**1**, **3** and **5**),[23,24] **2** occurs in a zwitterionic form. The hydrogen atoms H(1), H(5) and H(6) are located near to O(1), O(5) and O(6) oxygens (see Fig. 8) with a resultant formation of three strong intermolecular hydrogen bonds [2.446(2), 2.525(2) and 2.572(2) Å] (Table 7). A similar set of very short [2.398(3) Å] and short [2.511(3),

Table 7 Hydrogen bonds for compound **2** [Å and °]

D–H···A	*d*(D–H)	*d*(H···A)	*d*(D···A)	DHA
O(5)–H(5)···O(2^{i})	0.87(5)	1.61(5)	2.446(2)	160(5)
O(1)–H(1)···O(4^{ii})	0.73(5)	1.81(3)	2.525(2)	168(3)
O(6)–H(6)···O(3^{iii})	0.76(3)	1.84(3)	2.572(2)	160(4)
N(1)–H(2)···O(3^{iv})	0.85(2)	1.90(2)	2.710(2)	159(2)
C(3)–H(31)···O(4^{v})	0.89(3)	2.59(2)	3.142(2)	121(2)
C(3)–H(32)···O(5^{iii})	0.97(2)	2.62(2)	3.517(3)	154(2)
C(3)–H(33)···O(2^{vi})	1.01(3)	2.78(2)	3.427(3)	122(2)

Symmetry codes: (i) $x, -y + \frac{1}{2}, z + \frac{1}{2}$; (ii) $-x + 1, y + \frac{1}{2}, -z + \frac{1}{2}$; (iii) $-x, y - \frac{1}{2}, -z + \frac{1}{2}$; (iv) $-x, -y, -z$; (v) $-x + 1, y - \frac{1}{2}, -z + \frac{1}{2}$; (vi) $-x + 1, -y, -z$.

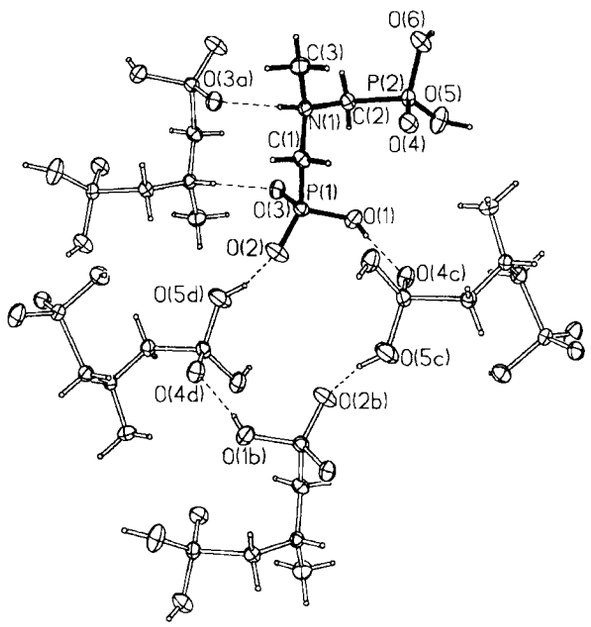

Fig. 9 Tetramer ($R_4^4(16)$ ring motif) formed by hydrogen bonds between phosphonate groups and dimer ($R_2^2(10)$ ring motif) formed by hydrogen bonds between phosphonate groups and imino atoms.

2.567(4) Å] hydrogen bonds was previously found in the crystal of *N*-ethyliminodimethylenediphosphonic acid **3**.[24]

Generally, the bond lengths in both phosphonic acid groups of the molecule are in a good agreement with those found earlier for compounds **1**, **3** and **5**. The P(2)–O(5) [1.5190(15) Å] distance is significantly shorter than a typical P–OH bond length. This fact can be explained by formation of a very strong hydrogen bond [2.446(2) Å] between the O(5) and O(2) with a resultant electron redistribution, which effects an elongation of the P(1)–O(2) bond and shortening of the P(2)–O(5) bond. A similar phenomenon has been observed for **3** where the corresponding P–O distance is 1.517(3) Å.

The angular disposition of the bonds around the phosphorus atom in each phosphonic acid group deviates significantly from that of a regular tetrahedron (Table 6) which is usually observed for phosphonate groups. Since the methyl group on the imino nitrogen is small the value of the C–N–C angle is very close to that in compound **1** [115.64(13), 115.0(3)°, respectively]. On the contrary, the bulky substituents in **3** and **5** lead to some decrease of the C(1)–N(1)–C(2) angle [113.1(3), 112.4(3)°, respectively]. The side-chain conformation of **2** is determined by the P(1)–C(1)–N(1)–C(2) and P(2)–C(2)–N(1)–C(1) torsion angles (Table 6) which are equal to −57.0(2) and −69.1(2)°. Consequently the molecule is of *gauche-gauche* conformation. The same conformation was found for compound **3**, for which the corresponding angles are −68.0 and −83.9°. In contrast, the side-chains in **1** and **5** appear in *gauche-trans* [60.8, 179.4°] and *trans-gauche* [−179.1, 50.5°] conformations. Therefore, the methyl group is in *trans-gauche* [173.8(1), 59.6(2)°] position in respect of both the P(1) and P(2) atoms. In the case of **3** and **5** the ethyl group and cyclohexyl ring assumed *gauche-trans* [59.9, 148.2 and 51.6, −179.4°, respectively] positions.

Both the molecular conformation and the position of the recognition sites are responsible for the unique 3-D arrangement of *N*-methyliminodimethylenediphosphonate. The end phosphonate groups serve both as hydrogen bond donor and hydrogen bond acceptor in order to form three short hydrogen bonds. From a supramolecular point of view, the first level molecular organisation can be perceived as centrosymmetric tetramer formation realised by the two strongest hydrogen bond interactions O(5)–H(5)···O(2) [2.446(2) Å] and O(1)–H(1)···O(4) [2.525(2) Å] and formally described with a graph set $R_4^4(16)$[25] (see Fig. 9). Such an arrangement of four phosphonate groups is indeed a very rare phenomenon in the crystallographic literature.[26,27] This tetramer can be considered as a basic building unit generating the whole three-dimensional crystal structure. The imino hydrogens H(2) of one tetramer access the O(3) oxygens of four neighbouring inversion related molecules *via* hydrogen bonded ring motifs $R_2^2(10)$ [N(1)–H(2)···O(3), 2.710(2) Å]. The O(6)–H(6)···O(3) hydrogen bond [2.572(2) Å] realises the linkages between the tetramer units in the third direction. The three-dimensional organisation is additionally stabilised by three weak C–H···O hydrogen bonds (see Table 7). The size of the CH_3 substituent on the imino nitrogen seems to be crucial for the conformation of **2** which evolves into a tetramer formation.

Conclusion

The high complexation efficiency of iminodimethylenediphosphonic acids derives from the presence of the dinegatively charged phosphonate groups and the strong metal binder, which is the imino nitrogen. It results in the formation of various complexes with zinc(II), magnesium(II) and calcium(II) ions. The significant preference for an equimolar stoichiometry is a common feature of these systems. The amount of the tridentate species as well as the pH region where they appear strongly depend upon the cation binding ability towards the nitrogen donor (Zn > Mg ⩾ Ca). Thus, the tridentate complexes with two joined five-membered chelate rings predominate in solutions at pH of about 7–11 for the majority of the zinc systems. On the contrary, Ca^{II} and Mg^{II} prefer a pure phosphonate co-ordination.

The only exception is compound **8**, in which the tetrahydrofuryl oxygen atom is sterically accessible for an additional effective binding to the metal ion. Both the potentiometry and the NMR titration data reveal that the involvement of the tetrahydrofuryl oxygen in the zinc(II) complexation strongly promotes nitrogen binding which results in a tetradentate coordination not only in [ZnL], but also in the protonated complex (Scheme 1). Moreover, the considerable affinity of Ca^{II}

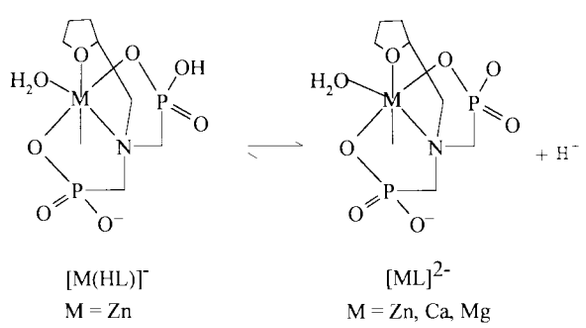

Scheme 1 The proposed structures of the $[M(HL)]^-$ and $[ML]^{2-}$ complexes of compound **8**.

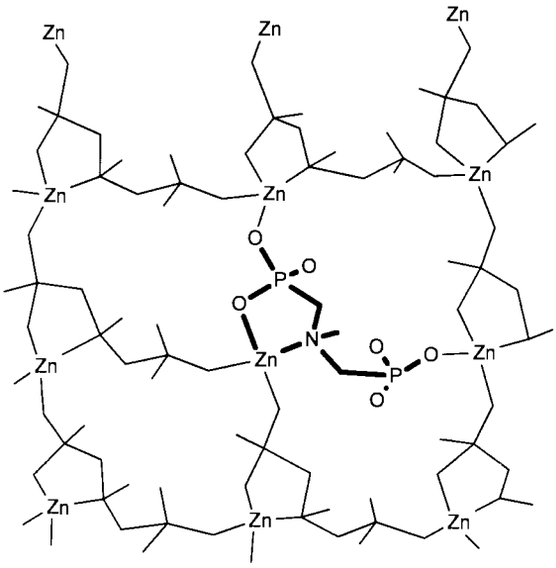

Fig. 10 The proposed model of zinc(II) binding in the Zn^{II}–**2** layered system.

for the tetrahydrofuryl oxygen seems to facilitate even Ca^{II}–N bond formation. Such binding, although weak (usually 2.5–2.7 Å) and rather seldom, has been proved by the crystal structures of several calcium complexes.[28]

However, the most intriguing results were obtained for the zinc(II)–**1** and –**2** systems. Based on the NMR spectra, the species formed in these solutions are characterised by an equimolar Zn^{II} to ligand stoichiometry and by the chemically distinctive methylenephosphonate groups. The NMR spectra reveal a slow (on the NMR timescale) exchange, that we considered as resulting from the formation of polymeric species. The lack of this phenomenon in the solutions of Ca^{II} and Mg^{II} allows us to suppose that the Zn–N binding is a key factor required for the appearance of new species.

Two possible complexation mechanisms can be considered in order to explain our experimental data. We can speculate that the observed zinc species are fairly similar to those of Cu^{II} with compound **3** and/or *N*-phosphonomethylglycine where tridentately co-ordinated copper(II) units are connected through the phosphonate oxygen in order to form polymeric chains.[29] Another possible mechanism is to consider the formation of two-dimensional frameworks with Zn^{II}. The literature data also indicate that in the solid state zinc(II) readily forms layered phosphonates with either tetrahedral[30,31] or octahedral[31,32] environments for the metal ion. Our model assumes that the chelated Zn^{II}–**2** (**1**) units form one-dimensional chains *via* co-ordination bonds from one phosphonate group. These chains further cross-link *via* co-ordination of the second phosphonate group towards the Zn^{II} of adjacent chains, thus forming a two-dimensional layer.

In fact, in the case of Zn^{II}–**2** (Fig. 10) we can presume formation of the tetrameric units as a scaffold for two-dimensional ligand-ion arrangement (compare with the crystallographically confirmed tetrameric units formed by **2**, Fig. 9). Under neutral and slightly alkaline conditions the hydrogen bonds start to break with subsequent release of the protons involved in them. As a consequence, the electron lone pairs on the phosphonate oxygens are ready to accept metal ions. Additionally, a ligand flipping with resulting chelation *via* the nitrogen atom is allowed due to the size and electron configuration of the Zn^{II}. Therefore, the tetrameric units formed in Zn^{II}–**2** can be considered as a consequence of the hydrogen bond breaking and ligand deprotonation with resultant replacement of the protons by Zn^{II}. This complexation mechanism seems to be more plausible compared to the first. Bulky substituents on N in compounds **3**–**8** impose steric confinement, and thus disfavour the layer formation. On the other hand the small substituent in **1** (the hydrogen atom) is not removable from the nitrogen and probably participates in a hydrogen bond which changes the system configuration, contravening to some extent the layer formation (Fig. 6(b)).

The dilution of systems Zn^{II}–**1** and Zn^{II}–**2** leads to disintegration of the layered organisation and formation of well characterised mononuclear complexes which additionally supports our conception that all the observed phenomena for the studied systems originate in the existence of polymeric species.

Acknowledgements

The authors wish to express their thanks to dr hab. Veneta-Videnova-Adrabińska from University of Technology of Wrocław for stimulating discussion during the preparation of the manuscript. The work was financially supported by the Polish State Committee for Scientific Research, KBN (grant no. 2P30305507).

References

1 S. J. Westerback and A. E. Martell, *Nature* (*London*), 1956, **178**, 321; C. V. Banks and R. E. Yerick, *Anal. Chim. Acta*, 1959, **20**, 301; E. N. Rizkalla and M. T. M. Zaki, *Talanta*, 1979, **26**, 506; I. Lazar, A. D. Sherry, R. Ramasamy, E. Brucher and R. Kiraly, *Inorg. Chem.*, 1991, **30**, 5016; G. B. Bates, E. Cole, D. Parker and R. Kataky, *J. Chem. Soc.*, *Dalton Trans.*, 1996, 2693; M. Dyba, M. Jeżowska-Bojczuk, E. Kiss, T. Kiss, H. Kozłowski, Y. Leroux and D. El Manouni, *J. Chem. Soc.*, *Dalton Trans.*, 1996, 1119; T. Ichikawa and K. Sawada, *Bull. Chem. Soc. Jpn.*, 1997, **70**, 2111; P. Buglyo, T. Kiss, M. Dyba, M. Jeżowska-Bojczuk, H. Kozłowski and S. Bouhsina, *Polyhedron*, 1997, **16**, 3447.
2 G. Schwarzenbach, H. Ackerman and P. Ruchstuhl, *Helv. Chim. Acta*, 1945, **28**, 1133; 1949, **32**, 1175.
3 M. M. Reddy and G. H. Nancollas, *Desalination*, 1973, **21**, 61; M. M. Reddy, *J. Cryst. Growth*, 1977, **41**, 287; G. H. Nancollas and K. Sawada, *J. Pet. Technol.*, 1982, 645; E. N. Rizkalla, *Rev. Inorg. Chem.*, 1983, **5**, 223.
4 *The Herbicide Glyphosate*, eds. E. Grossbad and D. Atkinson, CRC Press, Boca Raton, FL, 1989; G. Forlani, B. Lejczak and P. Kafarski, *Pestic. Biochem. Physiol.*, 1996, **55**, 180; P. Kafarski, B. Lejczak, G. Forlani, R. Gancarz, C. Torreilles, J. Grembecka, A. Ryczek and P. Wieczorek, *J. Plant Growth Regul.*, 1997, **16**, 153; V. Oberhauser, J. Gaudin, R. Fonne-Pfister and H.-P. Schär, *Pestic. Biochem. Physiol.*, 1998, **60**, 111.
5 K. Moedritzer and R. R. Irani, *J. Org. Chem.*, 1966, **31**, 1603; M. Soroka and P. Mastalerz, *Pol. J. Chem.*, 1976, **50**, 661; J. Oleksyszyn, E. Gruszecka, P. Kafarski and P. Mastalerz, *Monatsh. Chem.*, 1982, **113**, 1138.
6 G. Gran, *Acta Chem. Scand.*, 1959, **4**, 599.
7 M. Molina, C. Melios, J. O. Tognalli, L. C. Luchiari and M. Jafelicci, jun., *J. Electroanal. Chem. Interfacial Electrochem.*, 1979, **105**, 237.
8 P. Gans, A. Sabatini and A. Vacca, *J. Chem. Soc.*, *Dalton Trans.*, 1985, 1195.
9 G. M. Sheldrick, *Acta Crystallogr.*, *Sect. A*, 1990, **46**, 467.
10 G. M. Sheldrick, SHELXL 93, Program for the Refinement of Crystal Structures, University of Göttingen, 1994.
11 B. Kurzak, A. Kamecka, K. Kurzak, J. Jezierska and P. Kafarski, *Polyhedron*, 1998, **17**, 4403.
12 K. Sawada, T. Kanda, Y. Naganuma and T. Suzuki, *J. Chem. Soc.*, *Dalton Trans.*, 1993, 2557; K. Sawada, T. Ichikawa and K. Uehara, *J. Chem. Soc.*, *Dalton Trans.*, 1996, 3077; K. Sawada, T. Araki and T. Suzuki, *Inorg. Chem.*, 1987, **26**, 1199; K. Sawada, T. Miyagawa, T. Sakaguchi and K. Doi, *J. Chem. Soc.*, *Dalton Trans.*, 1993, 3777.
13 T. Kiss, J. Balla, G. Nagy, H. Kozłowski and J. Kowalik, *Inorg. Chim. Acta*, 1987, **138**, 25; B. Kurzak, E. Matczak-Jon and M. Hoffmann, *J. Coord. Chem.*, 1998, **43**, 243.
14 W. Bal, I. Bertini, H. Kozłowski, R. Monnani, A. Scozzafava and Z. Siatecki, *J. Inorg. Biochem.*, 1990, **40**, 227.
15 M. Jeżowska-Bojczuk, T. Kiss, H. Kozłowski, P. Decock and J. Barycki, *J. Chem. Soc.*, *Dalton Trans.*, 1994, 811.
16 R. P. Carter, R. L. Carrol and R. R. Irani, *Inorg. Chem.*, 1967, **6**, 939.
17 M. M. Olmstead, W. J. Grigsby, D. R. Chacon, T. Hascall and P. P. Power, *Inorg. Chim. Acta*, 1996, **251**, 273.
18 T. E. Glassman, A. H. Liu and R. R. Schrock, *Inorg. Chem.*, 1991,

30, 4723; P. Sobota, M. Wróblewska, S. Szafert and T. Głowiak, *J. Organomet. Chem.*, 1994, **481**, 57; C. K. Vishwanath, N. Shamala, K. R. K. Easwaran and M. Vijayan, *Acta Crystallogr., Sect. C*, 1983, **39**, 1640; B. K. Toeplitz, A. I. Cohen, P. T. Funke, W. L. Parker and J. Z. Gougoutas, *J. Am. Chem. Soc.*, 1979, **101**, 3344.
19 E. Matczak-Jon, B. Kurzak, W. Sawka-Dobrowolska, B. Lejczak and P. Kafarski, *J. Chem. Soc., Dalton Trans.*, 1998, 161; E. N. Rizkalla and G. R. Choppin, *Inorg. Chem.*, 1983, **22**, 1478.
20 J. Dekker, J. Boersma and G. J. M. van der Kerk, *J. Chem. Soc., Chem. Commun.*, 1983, 553; F. Bottomley, E. C. Ferris and P. S. White, *Acta Crystallogr., Sect. C*, 1989, **45**, 816.
21 W. McFarlane, *J. Chem. Soc. A*, 1968, 1715; S. Mazzini, R. Mondelli, E. Ragg and L. Scaglioni, *J. Chem. Soc., Perkin Trans. 2*, 1995, 285; W. I. Jung, A. Staubert, S. Widmaier, T. Hoess, M. Bunse, F. Vanerckelens, G. Dietze and O. Lutz, *Magn. Reson. Med.*, 1997, **37**, 802.
22 C. K. Johnson, ORTEP II, Report ORNL-5138, Oak Ridge National Laboratory, Oak Ridge, TN, 1976.
23 L. M. Shkol'nikova, G. V. Polyanchuk, N. M. Dyatlova, T. Ya. Medved', I. B. Goryunova and M. I. Kabachnik, *Izv. Akad. Nauk SSSR, Ser. Khim.*, 1985, 1035.
24 B. I. Makaranets, T. V. Polynova, V. K. Bel'skii, S. A. Il'ichev and M. A. Porai-Koshits, *Zh. Strukt. Khim.*, 1985, **26**, 131.
25 M. C. Etter, J. C. McDonald and J. Bernstein, *Acta Crystallogr., Sect. B*, 1990, **46**, 256.
26 F. H. Allen, J. E. Davies, J. J. Gelloy, O. Johnson, O. Kennard, C. F. Macrae, E. M. Mitchell, G. F. Mitchell, J. M. Smith and D. G. Watson, *J. Chem. Int. Comput. Sci.*, 1991, **31**, 187.
27 J. Mazurek and T. Lis, *J. Mol. Struct.*, 1999, **474**, 143.
28 A. Taeb, H. Krischner and C. Kratky, *Z. Kristallogr.*, 1986, **177**, 263; M. L. Tul'chinskii, L. Kh. Minacheva, V. G. Sakharova, A. Yu. Toivadze and M. A. Porai-Koshits, *Koord. Khim.*, 1990, **16**, 1202; N. S. Poonia, R. Chandra, V. M. Padmanabhan and V. S. Yadav, *J. Coord. Chem.*, 1990, **21**, 167; A. F. Waters and A. H. White, *Aust. J. Chem.*, 1996, **49**, 87, 61; H. Schmidbaur, T. Bach, D. L. Wilkinson and G. Muller, *Chem. Ber.*, 1989, **122**, 1439; G. Hundal, H. Martinez-Ripoll, M. S. Hundal and N. S. Poonia, *Acta Crystallogr., Sect. C*, 1996, **52**, 789.
29 E. T. Clarke, P. R. Rudolf, A. E. Martell and A. Clearfield, *Inorg. Chim. Acta*, 1989, **164**, 59; B. I. Makaranets, T. N. Polynova, N. D. Mitrofanova and M. A. Porai-Koshits, *Zh. Strukt. Khim.*, 1991, **32**, 116.
30 D. M. Poojary, B. Zhang and A. Clearfield, *J. Am. Chem. Soc.*, 1997, **119**, 12550; S. Drumel, P. Janvier, D. Deniaud and B. Bujoli, *J. Chem. Soc., Chem. Commun.*, 1995, 1051; D. M. Poojary and A. Clearfield, *J. Am. Chem. Soc.*, 1995, **117**, 11278.
31 D. M. Poojary, B. Zhang, P. Bellinghausen and A. Clearfield, *Inorg. Chem.*, 1996, **35**, 5254; S. Drumel, P. Janvier, P. Barboux, M. Bujoli-Doeuff and B. Bujoli, *Inorg. Chem.*, 1995, **34**, 148; V. Penicaud, D. Massiot, G. Gelbard, F. Odobel and B. Bujoli, *J. Mol. Struct.*, 1998, **470**, 31.
32 K. J. Martin, P. J. Squattrito and A. Clearfield, *Inorg. Chim. Acta*, 1989, **155**, 7; B. Zhang, D. M. Poojary and A. Clearfield, *Inorg. Chem.*, 1998, **37**, 1844.

Paper 9/03997J